JOURNAL OF GEOPHYSICAL RESEARCH, VOL. 90, NO. C4, PAGES 7037–7043, JULY 20, 1985

A Numerical Study of the Roles of Subgyre-Scale Mixing and the Western Boundary Current on Homogenization of a Passive Tracer

DAVID L. MUSGRAVE

Department of Physical Oceanography, Woods Hole Oceanographic Institution, Massachusetts

A numerical model integrated the steady advection-diffusion equation by using a kinematic circulation with characteristics of a subtropical gyre, i.e., closed streamlines and western intensification. Homogenization of the interior concentration increased, and the gradients were forced to the boundaries as mixing, parameterized as eddy diffusion, decreased. As the western boundary current intensified, the value of the homogenized interior became closer to the southern boundary value. This indicated that cross-stream mixing was enhanced within the western boundary current. Tongues of high and low tracer concentration spiraled across streamlines toward the center of the gyre. These simulations will be helpful in the interpretation of lateral distributions of geochemical tracers, which are being generated by programs such as TTO.

1. INTRODUCTION

Chemical and physical oceanographers have recognized that the large-scale gyres characteristic of much of the general oceanic circulation are regions of homogeneous property fields and that property gradients are relegated to thin plumes at the outer edges of the gyres [*Sarmiento et al.*, 1982; *Keffer*, 1985]. However, the role of subgyre-scale mixing in the maintenance of a homogeneous interior may have been confused. One might conclude, erroneously, that greater mixing results in greater homogenization. In fact, greater mixing, as parameterized by higher eddy diffusivities, serves to smooth anomalies, and the large gradients near the edges of gyres would be less likely. *Young* [1984] indicates that the Western Boundary Current (WBC) can also increase the mixing characteristics of a gyre. The potential for diffusion to transport tracer across streamlines in the WBC increases as the width of the WBC decreases.

We used a steady circulation pattern with western intensification to examine the role of the WBC and subgyre-scale mixing on homogenization of a property within a gyre. We numerically integrated the advection-diffusion equation in a square, two-dimensional ocean by using a circulation pattern similar to *Stommel*'s [1948] solution for a wind-driven gyre. The tracer diffusivity and width of the WBC were varied over the relevant parameter space.

It might seem preferable to study tracer distributions in a full eddy-resolving general circulation model (GCM). Indeed, this is being done, but the present simple advection-diffusion model can be explored far more exhaustively than can a GCM. It is a useful complementary approach. The role of mixing in the WBC, for example, is sensitive to the Peclet number, boundary layer width, and the nature of the boundary conditions. The overall Nusselt number of the gyre (i.e, the net meridional flux of tracer compared to the purely diffusive flux) depends on these parameters in surprising ways. Explanation of this simpler model is a manageable task.

The most important result of this study was that a well-defined, homogeneous plateau of tracer developed in the interior of the gyre whose area increased with decreasing diffusive mixing. There was no homogeneous plateau for cases of very strong mixing. The role of the WBC in determining the concentration of the homogeneous plateau was also of interest. For a symmetric circulation, i.e., no western intensification, the tracer concentration of the homogeneous plateau was the average of the concentrations on the northern and southern boundaries, as expected. As the western intensification increased, the tracer concentration of the plateau approached the value on the southern boundary. This supported the notion that tracer concentrations along the outermost streamlines in the WBC, which acquired values near the concentration of the southern boundary, were increasingly mixed into the interior as the width of the WBC decreases.

Tongues of high and low tracer concentrations spiraled into the stagnation point of the circulation. This phenomena is inconsistent with the "Wustian"-type [*Wust*, 1935] conceptions that tongues are aligned with streamlines.

2. THE MODEL

The equation that describes the horizontal distribution of a tracer is

$$u\frac{\partial\theta}{\partial x}+v\frac{\partial\theta}{\partial y}=\kappa\left(\frac{\partial^2\theta}{\partial x^2}+\frac{\partial^2\theta}{\partial y^2}\right) \tag{1}$$

where θ is some conservative property, such as salinity; t is time; u is the east (x) velocity component; v is the north (y) velocity component; and κ is the horizontal diffusivity. We scaled the variables in (1) by using

$$\theta^* = 2(\theta-\theta_0)/\Delta\theta$$

$$(x^*, y^*) = (x/L, y/L)$$

$$(u^*, v^*) = (u/U, v/V)$$

where L is a characteristic horizontal dimension (taken here to be the width of the gyre basin), U a characteristic horizontal velocity, $\Delta\theta$ the difference between the concentration at the northern boundary and the concentration at the southern boundary, and θ_0 the average of the concentrations at those two boundaries. The new nondimensional equation is

$$Pe\left(u^*\frac{\partial\theta^*}{\partial x^*}+v^*\frac{\partial\theta^*}{\partial y^*}\right)=\frac{\partial^2\theta^*}{\partial x^{*2}}+\frac{\partial^2\theta^*}{\partial y^{*2}} \tag{2}$$

where $Pe = UL/\kappa$ is the Peclet number and is a measure of the relative importance of advection to diffusion. Increasing the eddy diffusivity decreases the Peclet number. Given a particu-

Paper number 5C0053.
0148-0227/85/005C-0053$05.00

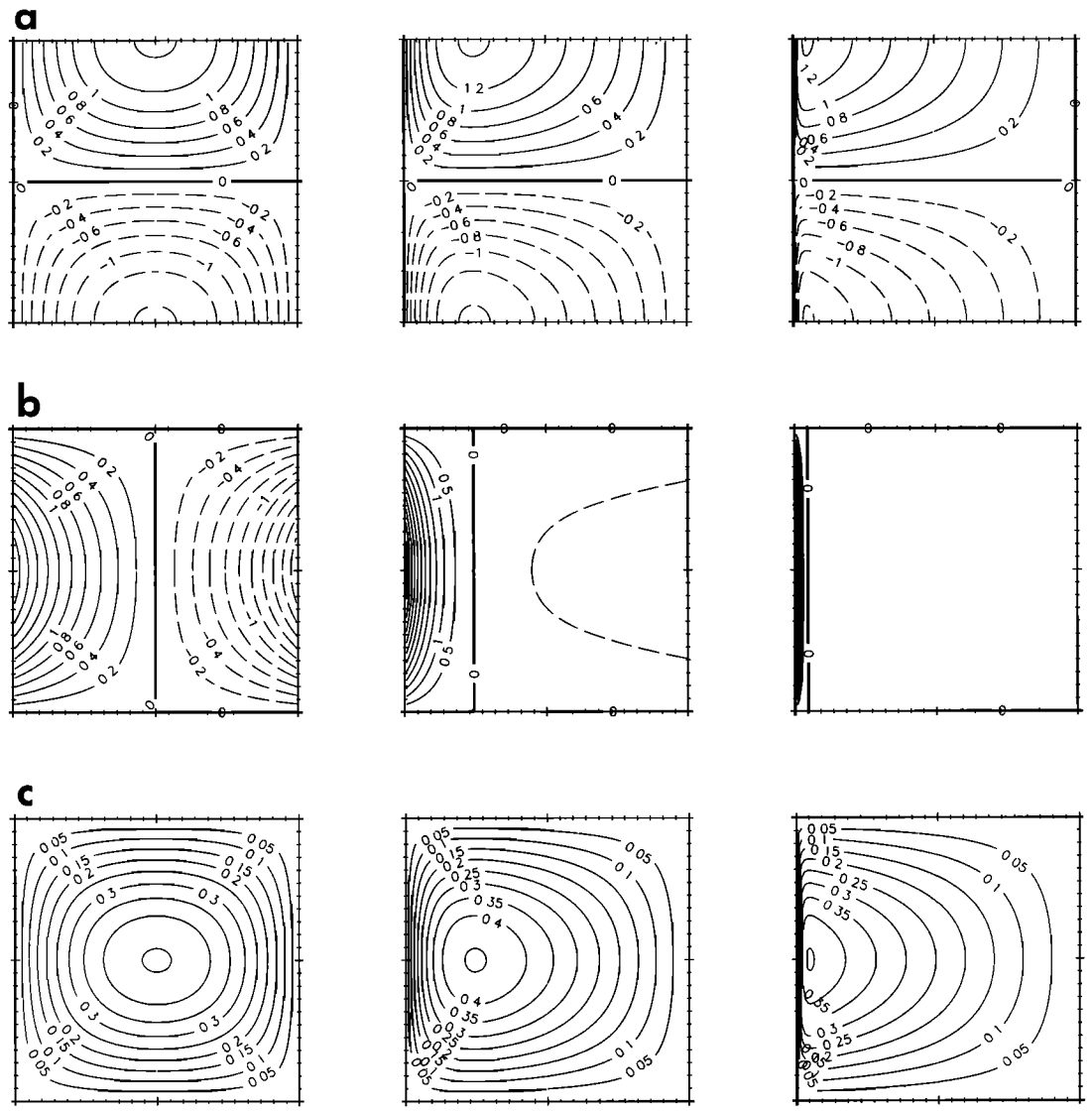

Fig. 1. (*a*) Zonal (u^*) and (*b*) meridional (v^*) velocities of the circulation for $\delta/L = 0.2$, 0.1, and 0.01 (left to right, respectively). Contours are solid, heavy, and dashed for positive, zero, and negative values, respectively. Maximum zonal velocities are a weak function of δ/L, but the meridional velocities in the WBC are inversely proportional to δ/L. No flow occurs across the boundaries. The maximum zonal velocities occur on the northern and southern boundaries at the longitude of the stagnation point. The zonal velocity is antisymmetric about $y^* = 1/2$ for all δ/L. The maximum meridional velocity occurs on the western boundary at $y^* = 1/2$ and is antisymmetric about $x^* = 1/2$ only when $\delta/L = 0.2$. Velocities were multiplied by factors of 10 (equivalent to dividing the tracer diffusivity by factors of 10) to obtain simulations with $Pe = 10$, 100, and 1000. (*c*) Streamlines (ψ = constant) of the circulation; $\psi = 0$ on the boundaries, and the maximum of the stream function is 0.454 for all δ/L, which yields a constant transport as δ/L varied.

lar set of boundary conditions and circulation pattern, the Peclet number determines the property field.

2*b*. *The Velocity Field*

We used a slight modification of the circulation scheme given by *Stommel* [1948]. The stream function was

$$\psi(x^*, y^*) = A \sin \pi y^*(c_1 e^{\lambda_1 x^*} + c_2 e^{\lambda_2 x^*} + 1)$$

$$\lambda_1 = \frac{-1 + \sqrt{1 + 4\pi^2\varepsilon^2}}{2\varepsilon} \qquad \lambda_2 = \frac{-1 - \sqrt{1 + 4\pi^2\varepsilon^2}}{2\varepsilon} \tag{3}$$

$$c_1 = \frac{1 - e^{\lambda_2}}{e^{\lambda_2} - e^{\lambda_1}} \qquad c_2 = -(1 + c_1)$$

The amplitude A was adjusted to give constant mass transport as ε was varied to change the intensity of the WBC. For $\varepsilon \ll 1$, $\varepsilon = \delta/L$, where δ is the width of the WBC. For $\varepsilon \gg 1$ the stream function is approximated by

$$\psi(x^*, y^*) = A \sin \pi y^*(-e^{-\pi(1-x^*)} - e^{-\pi(x^*)} + 1)$$

which is the stream function corresponding to a constant f (Coriolis frequency) ocean. The circulation pattern is symmetric about $x^* = 1/2$ in this case, and ε no longer gives an accurate approximation to δ/L, i.e., for $\varepsilon \gg 1$ in (3), δ/L is close to 0.2, as seen in Figure 1*a*. Thus, in the following experiments, we investigated the effect of the intensity of the WBC on property distributions by using $\varepsilon = 0.01$, 0.1, and 100.0, which yield $\delta/L = 0.01$, 0.1, and 0.2. The streamlines for these cases are shown in Figure 1, which also shows that the velocities in the WBC vary inversely as δ/L.

We arbitrarily assigned the value 1 to the characteristic

velocity U, which is an estimate of the magnitude of the interior velocity fields shown in Figure 1. (*Richardson and Mooney* [1975] took the U to be the maximum value of the stream function divided by L, which is a good approximation of the average southward velocities in the eastern part of the basin. This differs from the definition here by a factor of 0.454.) The circulation time t_c for a fluid element to go around the gyre one time is $O(L/U)$. In the absence of advection the diffusive time scale $t_d = O(L^2/\kappa)$ is a measure of the time for a tracer to diffuse across the gyre. Thus the Peclet number is the ratio of the diffusive time scale to the circulation time:

$$Pe = \frac{UL}{\kappa} = \frac{L^2/\kappa}{L/U} = \frac{t_d}{t_c}$$

We used Peclet numbers of 10, 100 and 1000 for this study.

2c. *Boundary Conditions*

In the following experiments the concentrations at the northern and southern boundaries were set to the constant values of 1 and -1, respectively. We set the eastern and western boundaries to no flux conditions.

2d. *Computations*

We started the integration on a 25 × 25 grid with transformed coordinates in both directions so that the large tracer gradients along the boundaries would be resolved (see appendix). We investigated the convergence as a function of resolution by doubling the number of grid points three times. We used a finite differencing scheme suggested by *Fiadeiro and Veronis* [1977]. Each simulation started with a field that linearly increased from -1.0 on the southern boundary to 1.0 on the northern boundary and iteratively converged to steady state by using the method of successive overrelaxation by points in alternating directions. Convergence to steady state was considered complete when the difference between the maximum and minimum Nusselt number at any latitude line was less than 1%. At any particular grid point the maximum variation of tracer concentration between iterations was about 1% when the convergence criterion was met.

For any given δ/L and Peclet number the Nusselt number obtained on the 25 × 25 grid was within 10% of the value on the 100 × 100 grid, which was within 1% of the value on the 200 × 200 grid. Thus convergence of the Nusselt number was guaranteed. Tracer concentrations converged more slowly than the Nusselt number as resolution was increased. For example the concentration at the stagnation point of the circulation varied by as much as 50% between the 25 × 25 and the 100 × 100 grid, and at the highest Peclet numbers the variation exceeded 10% between the 100 × 100 and the 200 × 200 grids. Nusselt numbers obtained on equally spaced grids that did not resolve the northern and southern boundary layers varied by more than 20% between the 100 × 100 and 200 × 200 grids for any given δ/L and Peclet number, which indicates the importance of using transformed coordinates. The number of iterations to steady state for any given resolution decreased as the Peclet number increased, which is one of the benefits of the *Fiadeiro and Veronis* [1977] differencing scheme.

3. RESULTS

Contour plots of the tracer fields are in Figure 2. In the purely diffusive case, i.e., $Pe = 0$ (not shown), the contour lines coincide with latitude lines. Increasing the Peclet number tended to wrap up the contours in the direction of circulation.

TABLE 1. Nusselt Number for Values of Pe and δ/L

	δ/L		
Pe	0.2	0.1	0.01
	This Work		
10	2.34/2.34	2.22/2.22	2.01/2.01
100	7.43/7.39	7.22/7.02	6.61/6.35
1000	23.3/23.4	22.4/22.2	20.1/20.1
	Fiadeiro and Veronis [1977]*		
2.46†	1.12/1.10		
6.61	1.74/1.90		
22.0	3.41/3.47		
110	7.53/7.78		
220	10.6/11.0		
881	21.0/21.9		

The values on the left were calculated from the simulations, and the values on the right are calculated from the Nusselt number at $Pe_0 = 10$, Nu_0, and the derived power law $Nu/Nu_0 \propto (Pe/Pe_0)^{1/2}$.

*These values are taken from Fiadeiro and Veronis, who used the stream function $\psi = \sin \pi x^* \sin \pi y^*$.

†The Peclet numbers from Fiadeiro and Veronis have been multiplied by the factor 0.454 in order to be consistent with the Peclet numbers in this study.

In the case of no WBC the contours were zonally and meridionally symmetric. A plateau of homogenized tracer values developed for $Pe = 100$ and 1000. This is most readily seen in the surface plots in Figure 3. As the Peclet number increased, the area of homogenized tracer increased in size, and the gradients became steeper near the northern and southern boundaries. This implied that the transfer (relative to the purely diffusive case, $Pe = 0$) across the diffusive layers at these boundaries increased as the Peclet number increased. Table 1 gives the Nusselt numbers for the nine cases. The meridional flux increased as the Peclet number increased, as expected. There was also a dependence of the Nusselt number on δ/L, although it was very small: for each Peclet number the Nusselt number decreased slightly as the WBC intensity increased.

The tracer concentration of the interior homogeneous regions for $Pe = 100$ and 1000 was a function of δ/L (Figures 3 and 4). When $\delta/L = 0.2$ the interior concentration was the average of the northern and southern boundary concentrations, as expected, given the symmetry of the circulation. As the WBC became more intense the interior concentration became closer to the southern boundary value (Table 2).

Figure 4 shows the concentration profile at $y^* = 1/2$ for the nine cases. These profiles emphasize the increasing homogenization in the interior and the expulsion of the gradients to the boundaries as the Peclet number increased. At the two higher Peclet numbers, tongues of high and low concentrations, seen as troughs and ridges in Figure 4, spiraled in across streamlines and point to the stagnation point of the circulation (Figure 2). The tongues became thinner as the Peclet number increased.

4. DISCUSSION

The tendency toward homogenization as the strength of the circulation increases has been studied by fluid dynamicists [e.g., *Roberts*, 1977]. Theories of free, thermal convection make use of this phenomena to obtain Nusselt numbers at high Rayleigh numbers (i.e., large buoyancy effects and hence large velocities). Similar considerations can be used to derive

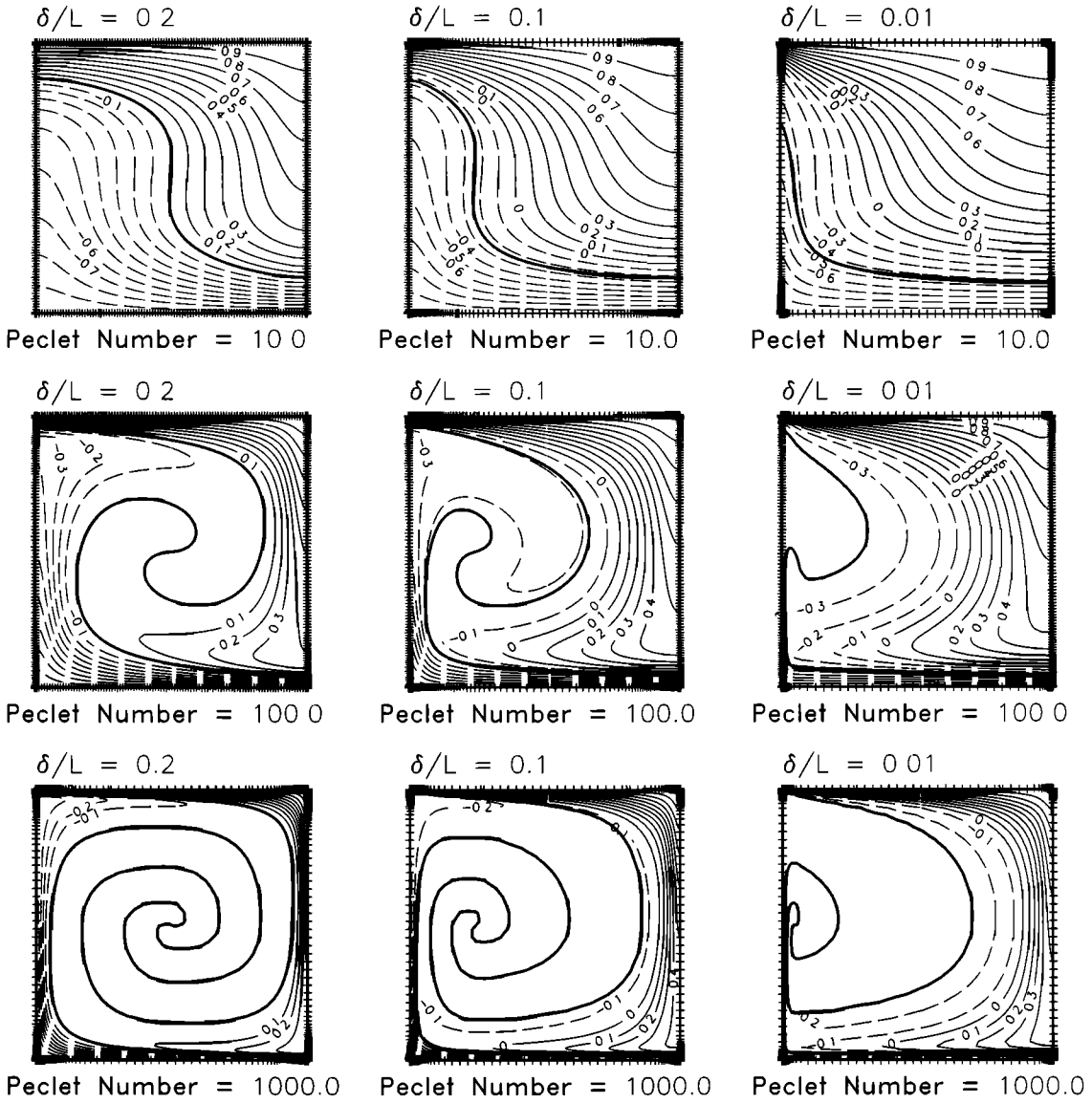

Fig. 2. Contour plots of the tracer fields for $Pe = 10$, 100, and 1000, and $\delta/L = 0.2$, 0.1, and 0.01. Contours are solid for nonnegative values and dashed for negative values. The heavy solid line is the contour that goes through the center of the circulation at ψ_{max}. The tracer fields were from simulation on 100 × 100 grids with transformed coordinates. The spacing of the grid points are indicated by tic marks along the boundaries: for higher Peclet numbers, more points were put near the northern and southern boundaries, and for lower δ/L, more points were put near the eastern and western boundaries. Contour plots from simulations on 200 × 200 grids were similar.

the proper scaling of the area of homogenization as a function of the Peclet number.

Consider the tracer boundary layer along the northern boundary. The width of the boundary layer increases as a fluid parcel moves from west to east along this wall. The thickness of the boundary layer is $l = \sqrt{\kappa t_{nb}}$, where t_{nb} is the time for the fluid element to traverse the width of the gyre at the northern boundary, i.e., t_{nb} is $O(L/U)$. Therefore the ratio l/L is $O(Pe^{-1/2})$. This scaling holds for $Pe \gg 1$ when the width of the boundary layer is much less than the width of the gyre. For the symmetric circulation an analogous boundary layer develops along the southern boundary. Plumes of slowly varying width, which are derived from the boundary layers along the northern and southern walls, are found along the meridional boundaries. We took the width of the ascending plume to be the distance from the western boundary to the first minimum to the east along the line $y^* = 1/2$, which is a good approximation to l (cf. Figure 2, $Pe = 100$ and 1000; $\delta/L = 0.2$). Figure 5 shows that this scaling applies to the symmetric circulation. Simple geometry can extend this argument to two dimensions to obtain the area of homogenization as a function of Pe. Visual inspection of Figure 3 indicated that similar considerations apply in an approximate way to the cases of western intensification.

The same boundary layer analysis can be used to scale the Nusselt number Nu as a function of the Peclet number. The width of the plume that descends along the eastern boundary is proportional to the width of the thermal layer along the northern boundary just before the flow turns south, which is given above as $l = \sqrt{\kappa L/U}$. Since the along-stream diffusive flux is negligible at the eastern boundary, then the dimensional flux of tracer, relative to the southern boundary concentration, is $(\theta_{nb} - \theta_{sb})lU/L$. The Nusselt number goes as this flux divided by the flux in the purely diffusive case, i.e., $\kappa(\theta_{nb}$

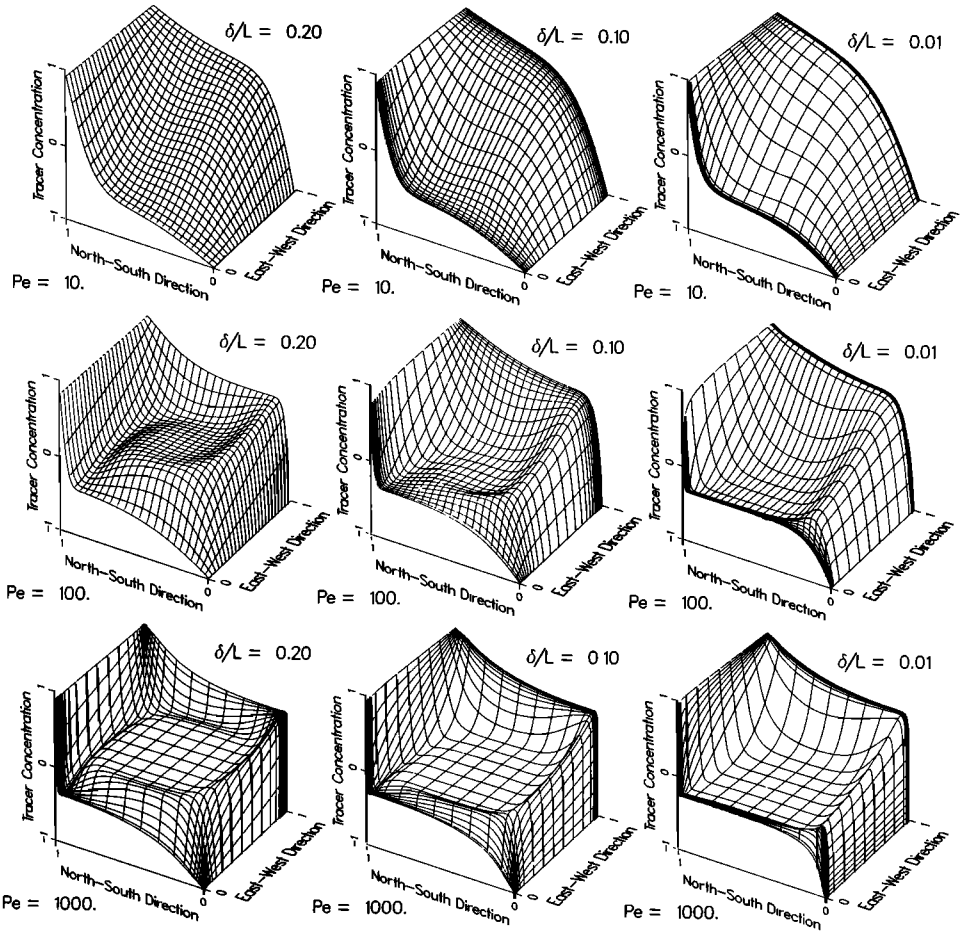

Fig. 3. Surface plots of the tracer fields. Every fourth line in each dimension of a 100 × 100 grid was traced. View is from the southwest corner of the gyre. Variation of δ/L and Pe as in Figure 2. The concentration of lines near the boundaries indicate the coordinate transformation. Homogenization occurs at $Pe = 100$ and 1000. At these Peclet numbers, enhanced mixing (for low values of $Pe\delta/L$) is seen as small differences between values on the western boundary and at the stagnation point ($Pe = 100$, $\delta/L = 0.1$, 0.01, and $Pe = 1000$, $\delta/L = 0.01$). When $Pe^{1/2}(\delta/L)^{1/2} \gg 1$ (lower left corner) a trough develops near the northern boundary.

$-\theta_{sb})/L$, which gives $Nu \propto Pe^{1/2}$. Table 1 shows that this relationship applied for these simulations. *Fiadeiro and Veronis* [1977] give the Nusselt numbers for a circulation with $\psi = \sin \pi x^* \sin \pi y^*$, which is very similar to the symmetric case in these simulations. The functional relationship between the Nusselt number and Pe for their simulations also support the above scale analysis. With proper scaling their Nusselt numbers fall on the same line as the symmetric calculations here (Figure 6).

Although the Nusselt number is mostly determined by the Peclet number, the trend as δ/L is varied was consistent, although slight: decreasing δ/L decreased the Nusselt number. Intensification of the velocity in the WBC as δ/L decreased was coincident with a more sluggish southward flow in the east. Thus the two effects are nearly offsetting in terms of transporting tracer. The consistent trend in the Nusselt number as a function of δ/L indicated that it is real, but we have not found a satisfactory argument for it.

TABLE 2. Concentrations of Tracer at the Stagnation Point of the Circulation for Simulations With Western Intensification

	δ/L	
Pe	0.1	0.01
10	−0.24	−0.42
100	−0.19	−0.34
1000	−0.13	−0.24

Converging streamlines in the southwest corner can decrease the distance between streamlines in the WBC. This gives diffusion a chance to increase the mixing between the values on the streamline defined by the western boundary and the value at the stagnation point. However, this enhanced mixing occurs only while a fluid element remains in the WBC: the increased velocity decreases the amount of time in the WBC. In a study of these two opposing effects, *Young* [1984] describes two limits depending on δ/L (assuming Pe is large). First, when $Pe\delta/L \gg 1$, diffusion is weak, even in the WBC, and an initial spot release of tracer must make several passes through the WBC before mixing across streamlines. Second, if $Pe\delta/L \ll 1$, then diffusion is strong in the WBC, and mixing occurs in one pass through the WBC.

These same limits also apply in these steady state simulations. In fact the ratio of the width of the diffusive plume within the WBC to the width of the WBC goes as $Pe^{1/2}(\delta/L)^{1/2}$ (in the limit that $Pe \gg 1$). This scaling can be obtained by realizing that the width of the ascending plume goes as $l_{wb} = \sqrt{\kappa L/v}$, where L/v is the time a fluid element spends in the WBC. Conservation requires $v\delta = UL$ so that

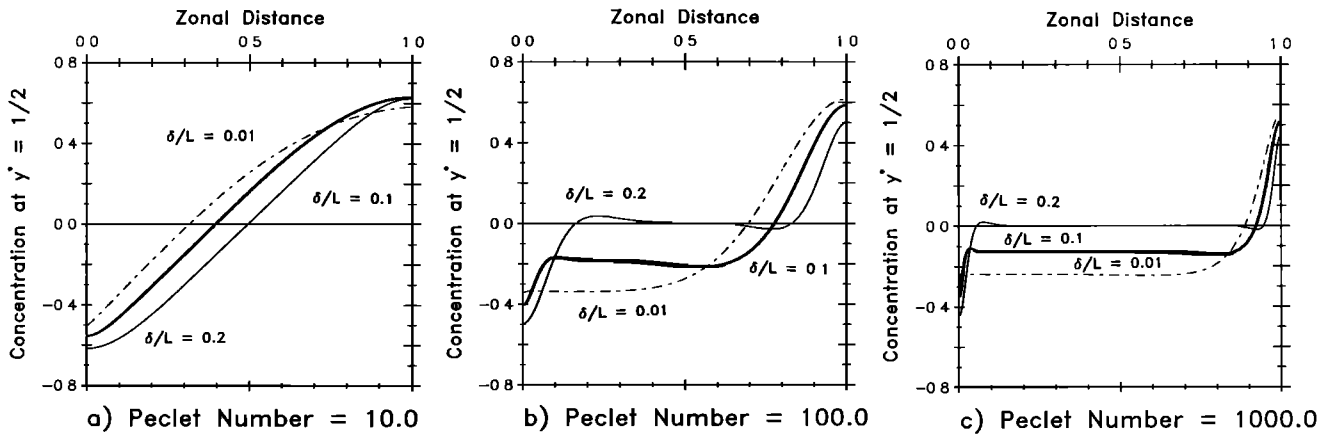

Fig. 4. Tracer concentration at mid-latitude ($y^* = 1/2$) for (*a*) $Pe = 10$, (*b*) $Pe = 100$, and (*c*) $Pe = 1000$. The solid, heavy, and dashed lines correspond to $\delta/L = 0.2$, 0.1, and 0.01, respectively. The region of homogenization increases for all δ/L as the Peclet number increases, and gradients are increased and forced to the boundaries. For $Pe = 100$ and 1000 the concentration of the homogeneous interior decrease as western intensification increases.

$l_{wb}/\delta = Pe^{-1/2}(\delta/L)^{-1/2}$. Again, $Pe^{1/2}(\delta/L)^{1/2} \gg 1$ implies weak diffusion in the WBC, and $Pe^{1/2}(\delta/L)^{1/2} \ll 1$ implies that a tracer is mixed into the interior as a fluid element passes through the WBC. The surface plots show that where this analysis holds (i.e., $Pe = 100$ and 1000), low values of $Pe\delta/L$ (upper right in Figure 3) yielded small differences between the western boundary values and the interior values. For example the concentration on the western boundary and at the stagnation point were very close for $\delta/L = 0.01$ and $Pe = 100$ ($Pe\delta/L = 1$). Tracer fields in the lower left of Figure 3 had large differences between the western boundary and the interior. It appears that a critical value of $Pe\delta/L \sim 10$ exists: for $Pe\delta/L < 10$ there was essentially no difference between the concentration at the western boundary and the interior and therefore no trough adjacent to the northern boundary where the flow exits from the WBC.

The enhanced mixing in the WBC for low values of $Pe\delta/L$ also affected the concentration of the homogenized interior. Since the tracer value along the western boundary was ultimately derived from the value along the southern boundary, the enhanced mixing served to decrease the concentration of the interior. Indeed, for $\delta/L = 0.1$ and 0.01 and $Pe = 100$ and 1000 the interior concentration can be ranked in order of increasing $Pe\delta/L$ (Table 2).

The results presented here on the effects of the WBC and subgyre-scale mixing on homogenization may be due to the boundary conditions we used. However, *Pedlosky* [1983] shows that homogenization of conservative tracers is a robust feature for small values of eddy diffusivity. Preliminary experiments with boundary conditions other than no flux along the eastern and western boundaries support this conclusion.

It seems intuitive that tongues of tracer concentration should somehow indicate flow lines. *Wust* [1935] used this reasoning to indicate the flow direction in the deep Atlantic. But as these simulations show, tongues actually crossed streamlines and pointed to the "center" or stagnation point of the gyre. Vertical exchange may alter this conclusion, but where lateral processes dominate, as in the subtropical ther-

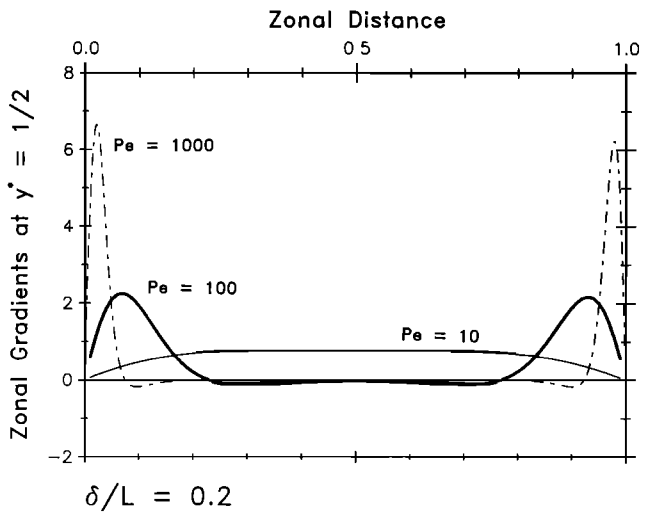

Fig. 5. Zonal gradients at mid-latitude ($y^* = 1/2$) for $\delta/L = 0.2$ (symmetric circulation) and $Pe = 10$ (solid), 100 (heavy), and 1000 (dashed). For the two higher Peclet numbers the linear distance to the first zero crossing was taken as the diffusive length scale l of the ascending plume. For $Pe = 100$ the length scale l_{100} (= 0.23) is $10^{1/2}$ (i.e., 3.16) times the length scale at $Pe = 1000$, l_{1000} (= 0.075), in accordance with the scale analysis developed in the text.

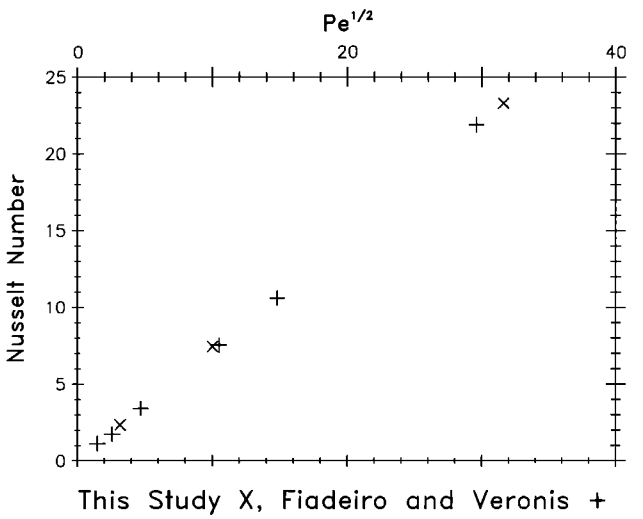

Fig. 6. Nusselt number as a function of $Pe^{1/2}$. The crosses (×) are data from this study ($\delta/L = 0.2$, symmetric circulation), and the plusses (+) are from *Fiadeiro and Veronis'* [1977] study. Their Peclet numbers have been adjusted to correspond with the definition of Pe in this study (Table 1).

mocline, one must be careful in drawing "Wustian"-type conclusions concerning tongues.

5. CONCLUSIONS

A numerical model was used to study the effects of mixing, as parameterized by eddy diffusion, and western intensification on the distribution of a conservative tracer in a gyre. Convergence of the solution was obtained by using a coordinate transformation such that all boundary processes were resolved.

Homogenization of the interior occurred for high Peclet numbers, and large gradients were found along the boundaries. This may be counterintuitive, since large Peclet numbers imply weak mixing. The concentration of the homogenized region is a function of the enhanced mixing caused by western intensification: the asymmetry of the flow with respect to the imposed boundary conditions causes the interior concentration to approach the value of the southern boundary. Tongues of tracer concentration cannot be used to infer flow lines; tongues spiral across streamlines toward the center of the gyre.

As more chemical distributions become available from the TTO (Transient Tracers in the Ocean) program, these simulations should help to explain the distributions of tracers mapped onto isopycnal surfaces within the thermocline of the subtropical gyre. Certainly, other processes will affect tracer distributions: interactions with biota, vertical exchange, eddies, various boundary conditions, and time dependency, to name a few. These are being incorporated into further modeling efforts in order to compare with these simulations. By this process we hope to simulate realistic distributions of tracers while learning about the processes most important in determining them.

APPENDIX

We used the following coordinate transformation in both the x and y direction:

$$\xi = x + \gamma\left[2 - \exp\left(\frac{-x}{\sigma}\right) + \exp\left(\frac{-(1-x)}{\sigma}\right)\right]$$

where ξ is the new coordinate, x is the old coordinate (nondimensional), γ is 1 or 0 to turn the transformation on or off, and σ is the e-folding scale for stretching near the boundaries. When σ is small the spacing in the interior in ξ is the same as in x; σ was varied independently in both directions in an empirical manner so that convergence of the solution to steady state at each level of resolution occurred within a few hundred iterations.

Acknowledgments. This work was completed while I received salary and benefit support through the Postdoctoral Scholar program at the Woods Hole Oceanographic Institution. The Center for Analysis of Marine Systems (CAMS) provided computer time for the development and implementation of the numerics. I gratefully acknowledge the constructive discussions with Bill Jenkins, Tom Keffer, and Peter Rhines. This is contribution number 5760 of the Woods Hole Oceanographic Institution.

REFERENCES

Fiadeiro, M. E., and G. Veronis, On weighted-mean schemes for the finite-difference approximation to the advection-diffusion equation, *Tellus, 29*, 512–522, 1977.

Keffer, T., The ventilation of the world's oceans: Maps of the potential vorticity field, *J. Phys. Oceanogr.*, in press, 1985.

Pedlosky, J., On the relative importance of ventilation and mixing of potential vorticity in mid-ocean gyres, *J. Phys. Oceanogr., 13*, 2121–2122, 1983.

Richardson, P. L., and K. Mooney, The Mediterranean outflow—A simple advection-diffusion model, *J. Phys. Oceanogr., 5*, 476–482, 1975.

Roberts, G. O., Fast viscous convection, *Geophys. Astrophys. Fluid Dyn., 8*, 197–233, 1977.

Sarmiento, J. L., C. G. H. Rooth, and W. Roether, The North Atlantic tritium distribution in 1972, *J. Geophys. Res., 87*, 8047–8056, 1982.

Stommel, H., The westward intensification of wind-driven ocean currents, *Eos Trans. AGU, 29*, 202–206, 1948.

Wust, G., Die Stratosphere, 1, *Wiss. Ergeb. Dtsch. Atl. Exped. "Meteor" 1925–1926, 6*, (2), 1935.

Young, W. R., The role of western boundary layers in gyre-scale ocean mixing, *J. Phys. Oceanogr., 14*, 478–483, 1984.

D. L. Musgrave, Department of Physical Oceanography, Woods Hole Oceanographic Institution, Woods Hole, MA 02543.

(Received August 27, 1984;
revised December 10, 1984;
accepted December 21, 1984.)